ACS Photonics

Article

pubs.acs.org/journal/apchd5

Plasmonic Tip Based on Excitation of Radially Polarized Conical Surface Plasmon Polariton for Detecting Longitudinal and Transversal Fields

Bayarjargal N. Tugchin,[†] Norik Janunts,[*,†] Angela E. Klein,[†] Michael Steinert,[†] Stefan Fasold,[†] Séverine Diziain,[†] Miguel Sison,[†,‡] Ernst-Bernhard Kley,[†] Andreas Tünnermann,[†,§] and Thomas Pertsch[†]

[†]Institute of Applied Physics, Abbe Center of Photonics, Friedrich-Schiller-Universität Jena, 07743 Jena, Germany

[§]Fraunhofer Institute for Applied Optics and Precision Engineering, 07745 Jena, Germany

S *Supporting Information*

ABSTRACT: We study experimentally the excitation of the radially polarized conical surface plasmon polariton (SPP) in a fully metal-coated conically tapered M-profile fiber which works as a "plasmonic tip" for the scanning near-field optical microscope (SNOM). This structure extends the Kretschmann configuration to the conical geometry. In this plasmonic tip, the radially polarized waveguide mode, propagating inside the fiber, resonantly excites the radially polarized SPP on the metal surface, which consequently gets confined at the apex where the field oscillates longitudinally along the tip axis. We also demonstrate the reverse process, where a longitudinal field excites the radially polarized SPP mode which then resonantly excites the radially polarized waveguide mode. This plasmonic tip combines the advantageous properties of near-field optical probes. Though, it has the shape of an apertureless SNOM tip, it can simplify the detection/excitation procedure and suppresses the background signal by its fiber-based design. Unlike the sharp apertureless SNOM tips that detects only the longitudinal field component or aperture SNOM tips that detect mostly the transversal component, the plasmonic tip detects both longitudinal and transversal field in collection mode and backward-scattering mode, respectively. The plasmonic tip, with further improvements, can become an advanced tool in SNOM due to its ability for background-free near-field detection, ease of operation, and higher conversion efficiency from far-field to near-field than conventional tips.

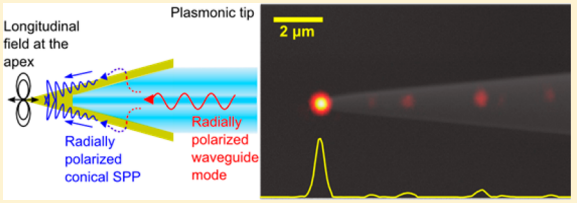

KEYWORDS: *plasmonic tip, radially polarized conical SPP, radially polarized fiber mode, longitudinal and transversal field, SNOM, M-profile fiber*

The biggest challenge for studying the optical properties of nano-objects arises in efficient delivery and detection of light to and from nanoscale regions. Surface plasmon polaritons (SPPs) help to overcome this limit.[1,2] It enables strong confinement and enhancement of electromagnetic energy below the diffraction limit of light in a variety of structures, particularly in tapered metallic structures with sharp edges or tips.[3,4] Being hybrid electromagnetic waves, SPPs comprise properties of transverse (photon) and longitudinal (plasmon) waves. When propagating in tapered metallic structures toward the sharp edges or apexes, longitudinal component of SPPs field becomes more pronounced.[5−14] This leads to a decrease of the wavelength, thus, allowing it to get localized at the tip apex and resulting in a highly confined and enhanced field at the apex with a strong longitudinal component.[5,7−9] This phenomenon is called SPP superfocusing, and in a metallic cone, it takes place only for the radially polarized SPP mode.[7,8] Tip-enhanced microscopy technique, which provides the highest spatial optical resolution among the optical detection methods, takes advantage of SPP localization at a nanoscale apex of a conical metallic tip.[15−23] The localization can be achieved either by exciting SPPs on a tip shaft[21−23] or simply by placing a tip in a focus of a tightly focused laser beam.[15−20] In the latter case, a focused radially polarized beam produces stronger longitudinal field enhancement at the apex than a linearly polarized one.[18−20] The excitation of SPPs on a tip shaft, which can be realized by incorporating a linear grating or photonic crystal structures in the shaft,[21−23] can improve the resolution and contrast of the optical images. Although these kinds of tip structures have high optical resolution, they have low conversion efficiency of energy from the far-field to the superfocusing SPP mode that generates a strong longitudinal field at the tip apex. To exploit the power of SPP superfocusing in scanning near-field optical microscopy (SNOM) applications, a tip design is required which is simple to produce, efficient in excitation of radially polarized SPP, applicable to sample and tip scanning, and robust in different application scenarios.

Theoretical studies showed that a high excitation efficiency of a radially polarized SPP on a metallic cone can be realized in a tapered and fully metal coated fiber via resonant coupling

Received: June 19, 2015
Published: October 5, 2015

DOI: 10.1021/acsphotonics.5b00339
ACS Photonics 2015, 2, 1468−1475

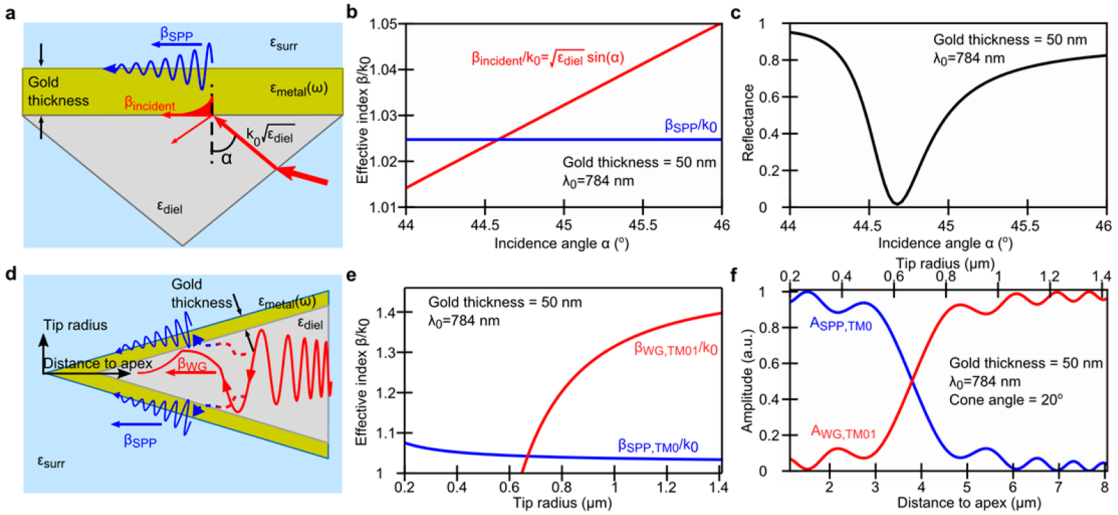

Figure 1. Comparison of Kretschmann geometries. (a–c) SPP excitation by the Kretschmann configuration in planar geometry. (d–f) SPP excitation by the Kretschmann configuration in cylindrically symmetric conical geometry. (a, d) Schemes of the planar and conical geometries. (b) Effective index (normalized propagation constant, β/k_0) vs incidence angle in the planar geometry. (c) Reflectance of the incident beam vs incidence angle in the planar geometry. (e) Effective indices (normalized propagation constant, β/k_0) vs tip radius in the cylindrical geometry for the radially polarized waveguide (WG) mode (TM_{01}) and the fundamental SPP mode (TM_0). (f) Amplitudes of the radially polarized WG mode (TM_{01}) and the fundamental SPP mode (TM_0) vs distance to apex in cylindrical geometry. In (b), (c), (e), and (f), calculations were obtained with the parameters λ_0 = 784 nm, ε_{surr} = 1, ε_{diel} = 2.13, and ε_{gold} = −20.95 + 1.68i.[39] In (b), (e), and (f), the imaginary part of ε_{gold} is neglected.

between a radially polarized waveguide (WG) and SPP modes.[24−31] To realize this tip experimentally, we suggest a structure (hereafter called "plasmonic tip") that can be fabricated by tapering and fully metal-coating an M-profile[32] fiber. This fiber has a special core design that guides cylindrical vector beams, particularly a radially polarized mode, with high modal purity. The plasmonic tip is essentially a Kretschmann configuration with cylindrically symmetric conical geometry, which enables efficient excitation of the radially polarized SPP mode on a metallic cone. We present an experimental realization of the plasmonic tip design and study systematically the SPP excitation processes taking place in the tip as well as its optical properties.

SPP Excitation by Kretschmann Configuration in Conical Geometry. For a better illustration of the SPP excitation in plasmonic tips, we compare schemes for exciting SPPs by the Kretschmann configuration in planar and conical geometries in Figure 1. To excite SPPs by the planar Kretschmann configuration, which consists of a glass prism coated by a thin metallic layer, the incidence angle of the excitation beam is varied until the phase matching condition is fulfilled (Figure 1a). Figure 1b shows calculated effective indices (β/k_0) of SPPs (blue line) and the incident beam (red line) depending on the incidence angle, where β is a propagation constant, and k_0 is a wave vector in vacuum. The crossing of lines indicates the phase matching angle. At this angle of incidence, energy transfers from a free space beam to SPPs by evanescent wave coupling through the metal layer, and as a result, the reflection decreases (Figure 1c). In Figure 1c, the dip in the calculated reflectance of the incidence beam indicates excitation of SPPs at the corresponding angle.[33]

For the conical Kretschmann configuration, we use a fully metal-coated conical dielectric waveguide (tapered optical fiber; cross section in Figure 1d). This geometry represents the plasmonic tip, which we study in this paper. Analytical models of this conical structure have been investigated previously,[24−27] and our theoretical treatment of the conical Kretschmann configuration is fully based on ref 25. Figure 1e shows calculations of the effective indices (β/k_0) of the radially polarized WG (TM_{01}, red line) and SPP (TM_0, blue line) modes (described by eqs 4 and 8 in refs 25). The effective indices of the WG and the SPP modes scale down and up with the fiber radius, respectively. Thus, the adiabatically decreasing radius enables phase matching between the WG and SPP modes at a certain radius. The conical Kretschmann configuration (plasmonic tip) supports the excitation of not only the fundamental TM_0 SPP mode but also excitation of higher order plasmonic modes,[34−36] whose profiles are not radially symmetric. Higher order SPP modes are excited via phase matching from higher order WG modes. These higher order SPP modes have cutoffs at different cone radii, and they radiate into the far field before reaching the tip-apex. Hence, only the fundamental SPP mode (TM_0, the superfocusing mode) reaches the tip apex, and only this mode can be excited by the radially polarized WG mode. In this paper, we focus on the excitation of the fundamental conical SPP mode (TM_0) that can reach the tip apex.

Figure 1f shows the evolution of the mode amplitudes (described by a system of the two coupled eqs 17 and 18 in ref 25, also see Supporting Information, S1) of the coupled radially polarized WG (red line) and SPP (blue line) modes along the propagation toward the tip. The WG mode amplitude decreases at the tip radius where the phase matching occurs while the SPP mode amplitude increases, indicating the resonant energy transfer from the WG mode to the SPP mode. The SPP excitation amplitude is over 90% for a tip with a gold coating of 50 nm and a full cone angle of 20° at a free-space excitation wavelength of λ_0 = 784 nm (see the blue line in Figure 1f). The coupling amplitude can also be well approximated by Landau–Zener formula (the details can be found in ref 25, see also Figure S1a in Supporting Information, S1). The excitation efficiency is as high as in the planar Kretschmann configuration. During the propagation to the apex (≈4 μm), the calculated loss of the radially polarized SPP is

DOI: 10.1021/acsphotonics.5b00339
ACS Photonics 2015, 2, 1468−1475

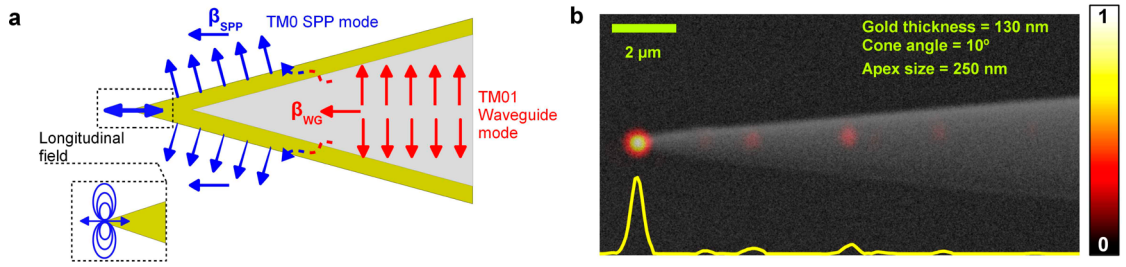

Figure 2. Side emission of a plasmonic tip in air. (a) Scheme of a longitudinal field at the tip apex, oscillating along the tip axis, generated by the radially polarized conical SPP (fundamental SPP mode TM_0). (b) Measured side emission pattern of a plasmonic tip with an apex radius of 125 nm (overlaid with the tip scanning electron microscope image). The apex emission is the consequence of the localized TM_0 SPP at the apex, resulting in a longitudinal field. The yellow curve shows the intensity profile of the side emission image along the central line of the tip. Side emission is measured with a 100×, NA = 0.75 objective (Zeiss).

about 22%. Thus, with this method, we can potentially deliver about 76% of the energy of the radially polarized WG mode in the tapered region to the longitudinally oscillating plasmonic field at the apex of the tip (the details of the calculations are shown in Supporting Information, S1). In comparison, in standard aperture SNOM tips, only 0.01% of the WG energy reaches the apex.[37,38]

Far-Field Side Emission of a Plasmonic Tip. The plasmonic tips, used in our study, are fabricated by tapering and fully gold coating M-profile fibers (Supporting Information, S2 and S3). We have chosen M-profile fibers due to their specially designed core, which allows us to guide the radially polarized mode reliably over long distances with high modal purity.[32] As explained in Methods, we first excite selectively the radially polarized mode in the fiber with the plasmonic tip. Then, we investigate an about 20 μm long section close to the apex of the tip by observing its far-field emission to the side.

The radially polarized WG mode (TM_{01}) can excite the fundamental conical SPP mode (TM_0) due to the non-orthogonality and phase matching between the WG and SPP modes. The longitudinal electrical field vector of the TM_0 SPP mode increases as it approaches the tip apex. Eventually, it behaves like a longitudinal dipole oscillating (along the tip axis) at the apex,[24] which results in strong far-field emission to the side (Figure 2a). Therefore, the side emission from the tip apex indicates the excitation of the fundamental conical SPP mode. The sharper the tip is, the stronger the longitudinal field at the apex is, consequently, the stronger the emission to the side is. Here, we have to note that, for sharp tips, the cone angle should not be very small; otherwise, the SPP propagation loss can overwhelm the field enhancement, making the SPP localization at the apex insignificant.[7,40] The connection between the fundamental conical SPP and the longitudinal field at the apex will be investigated further in this article.

Figure 2b shows a typical side emission pattern of a plasmonic tip, which has an apex radius of 125 nm, a gold thickness of 130 nm, and a full cone angle of 10°, overlaid with the tip scanning electron microscope image. The apex side emission has been demonstrated before in an electrochemically etched ultrasharp gold tip with an apex size of 20 nm.[22,23,41] Although the apex size of our plasmonic tip is large compared to the electrochemically etched tips, the presence of the longitudinal field is well observable.

A strong longitudinal field can also be observed in a focused radially polarized beam in free space.[42] When focusing a radially polarized beam with a high numerical aperture objective, the longitudinal field component increases toward the focus and it dominates over the transversal field component in the focus.[42] We observed a similar effect also for the plasmonic tips. The polarization-resolved side emission patterns of the plasmonic tip show that the emission is polarized longitudinally (Supporting Information, S5).

Apart from the apex emission, we observed weak spots away from the apex (see the yellow intensity profile curve of the side emission in Figure 2b), which are due to cutoffs of higher order SPP modes and perhaps also a bit of higher order WG modes. We checked the quality of the metal coating to make sure that it is free of imperfections that can cause strong scattering of SPP before they reach the apex. We did this check by cross-sectioning the tips and performing scanning electron microscopy imaging of the metal layer (see Figure S2 in Supporting Information). Higher order SPP modes reach cutoff at different radii of the tip away from the apex and radiate to far-field.[34−36]

Near-Field Analysis of a Plasmonic Tip Apex. As we mentioned above, the strong emission from the plasmonic tip apex to the side is related to the longitudinal field. To conclusively ensure its existence at the apex, we probed the near-field of the tip by investigating the planar SPPs excited by the plasmonic tip on a planar metallic surface in a SNOM setup. We placed the plasmonic tip perpendicularly to the planar gold surface to excite SPPs on it and analyzed their propagation directions by scattering them into the far-field. To scatter the planar SPPs in the far-field in normal direction, a bull's eye grating, consisting of a disk surrounded by periodic annular slits, was milled into the gold film (Figure 3a, see Methods). Since the longitudinal electric field at the apex, oscillating along the tip axis, is perpendicular to the planar gold surface, the planar SPPs, excited on the planar surface, have a radially polarized longitudinal component (parallel to the grating surface) that is radially symmetric with respect to the tip axis.[43] Therefore, the field distribution of the planar SPPs can be described by the Hankel function of zeroth order (Supporting Information, S6), which is a cylindrically symmetric function. The time-snapshot of SPP field ($\mathcal{R}e[E_z]^2$) on the gold surface has been calculated and is shown in Figure 3b.

We first obtained a topographic image of the grating (Figure 3c) by scanning it with a plasmonic tip. The image did not show any major imperfections in the grating. Then, the plasmonic tip was positioned in the center of the disk about 20 nm above the gold surface. The planar SPPs, excited by the plasmonic tip, propagate toward the grating and is scattered by the grating. The far-field image of the scattered planar SPPs, recorded by an inverted microscope and a camera (lower part of the experimental setup in Figure 3a), shows a bright ring

DOI: 10.1021/acsphotonics.5b00339
ACS Photonics 2015, 2, 1468−1475

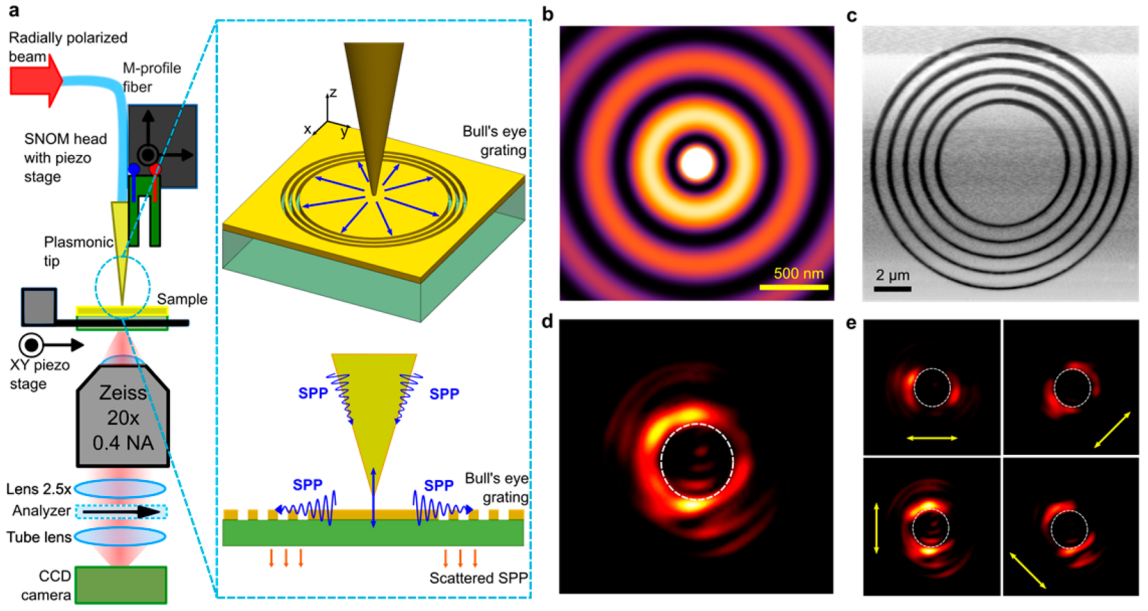

Figure 3. Excitation of a radially polarized planar SPP by a plasmonic tip. (a) Experimental setup that we use to position the tip at the center of a bull's eye grating and study the radially polarized planar SPP. (b) Calculated time-snapshot of SPP field ($\mathcal{R}e[E_z]^2$) of the radially symmetric planar SPP described by the Hankel function of 0th order (details in Supporting Information, S6). (c) Topographic image of the bull's eye grating recorded by the plasmonic tip. (d) Recorded charge coupled device (CCD) image of the SPP scattered by the bull's eye grating. The innermost groove is indicated by a white dashed circle. (e) Light scattered by the grating, imaged at different orientations of the polarization analyzer's transmission axis in front of the CCD camera. The transmission axis is indicated by yellow arrows, and the innermost groove is indicated by white dashed circles.

(Figure 3d). To check whether the scattered image originates from the planar SPPs, we retracted the tip about 4 μm, which resulted in vanishing of the bright ring at the location of the innermost grooves. This fact confirms that the bright ring originates from the planar SPPs generated by the apex near-field. The radially asymmetric patterns can be caused by scattering (by the grating) of the far-field emission originating from the tip's shaft (see previous chapter), slight off-center positioning of the tip, and probably also tiny tilt of the tip. Figure 3e shows the images taken with a polarization analyzer placed in front of the charge-couple device (CCD), where the analyzer transmission axis is indicated by yellow arrows and the innermost groove with white dashed circles. Since the images have two-lobe patterns that are oriented along the analyzer's transmission axis, one can claim that the far-field beam generated by the grating is radially polarized. Hence, we can deduce that the longitudinal component of the planar SPPs, excited by the plasmonic tip, is also radially polarized and radially symmetric.

Detection with a Plasmonic Tip via Radially Polarized Conical SPP. The existence of a longitudinal field at the apex of the plasmonic tip, when it is illuminated through the fiber, implies that the plasmonic tip will be mostly sensitive to the component of the external field that is parallel to the tip axis when used for near-field detection. To study the detection characteristics of a plasmonic tip, we scanned the tip over tightly focused linearly (HE_{11}, Gaussian shape) and radially (TM_{01}, doughnut shape) polarized beams and monitored the "transmitted" as well as the "backscattered" signals (see Figure 4a and Methods). The term "transmitted" refers to the signal detected by the plasmonic tip through the fiber, and the term "backscattered" denotes the signal that is scattered backward into free space and collected by the focusing objective.

The experimental results are shown in Figure 4b: the images of the "backscattered" signals are in the first column; and those of the "transmitted" signal are in the second column. The images for the radially polarized excitation beam (TM_{01}) are in the first row, and the images for the Gaussian excitation (HE_{11}) are in the second row. When compared with the analytical calculations[44−46] of the transversal and longitudinal components of the focused beams (Figure 4c), our experimental results demonstrate that the measured "transmitted" signals correspond to the longitudinal and the "backscattered" ones to the transversal field component of the focused excitation beams. Consequently, we conclude that the plasmonic tip is sensitive to the longitudinal field acting as an apertureless tip in collection mode and is sensitive to the transversal field in backscattering mode (when the scattering direction is parallel to the tip axis). In comparison, conventional sharp apertureless scattering SNOM tips are sensitive only to the longitudinal field, and fiber-based circular aperture SNOM tips are reported mostly to be sensitive to the transversal field (see also refs 47 and 48).

At the focus, the transversal field component of the calculated Gaussian beam is about 10× stronger than the longitudinal field component. The two-lobe pattern in the "transmitted" image of the scanned Gaussian beam emphasizes that there is no direct transmission or photon tunneling across the metallic film; otherwise, we would have detected a Gaussian-shaped image in transmission due to the dominant transversal field component.

The difference between the measured and the calculated images is caused by the fact that the scanning plane of the tip is not perfectly perpendicular to the beam axis (Supporting Information, S7). The tip apex size (~250 nm) also influences the recorded images: the full-width at half-maximum (fwhm) values of the focus in the transmission signals are slightly larger than the fwhm values of the focus in the calculated focus images. Comparison of the top two images in Figure 4b obtained for TM01 mode suggests us that the transmitted

DOI: 10.1021/acsphotonics.5b00339
ACS Photonics 2015, 2, 1468−1475

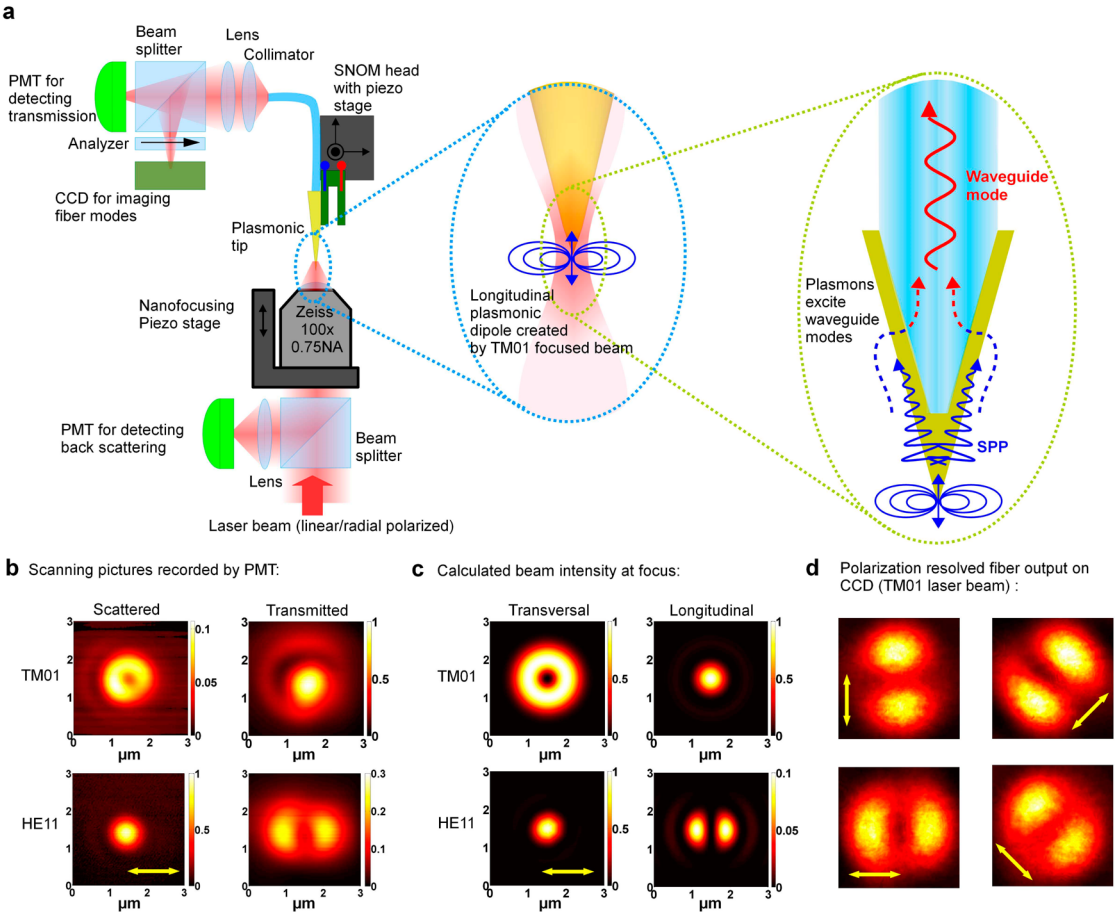

Figure 4. Radially polarized conical SPP excited by a longitudinal field at the tip apex. (a) Experimental setup. The focused beam excites a longitudinal field at the apex of the plasmonic tip which serves as a source of a radially polarized conical SPP originating from the apex. The SPP propagating away from the apex resonantly couples to the waveguide mode which can be detected and analyzed at the free end of the fiber. PMT and CCD denote photomultiplier tube and charge coupled device, respectively. (b) Measured "backscattered" (first column) and "transmitted" (second column) images of the focused radially (TM_{01}, first row) and linearly polarized (HE_{11}, second row) beams. (c) Calculated intensities of the transversal and longitudinal components of the focused beams. (d) CCD images of the waveguide mode, when the plasmonic tip is positioned in the center of the focused radially polarized beam (yellow arrows indicate the transmission axis of the polarization analyzer). These images show that the fiber mode is radially polarized.

signal (collected by the tip) is 10× stronger than the backscattered one. Whereas, for the HE11 mode (lower two images in Figure 4b), the situation is reversed: the back-scattering signal is 3× stronger than the transmitted one.

To analyze the excited fiber mode, the plasmonic tip is placed in the focus of the radially polarized beam, and the out-coupled beam from the fiber is imaged on a CCD. The polarization-resolved images in Figure 4d show that the WG mode emitted from the fiber is radially polarized. Since there is no direct tunneling through the metal layer (as we stated shortly above), we can claim that the radially polarized conical SPP (TM_0), on the outer surface of the conical tip, excites this WG mode. The energy of the radially polarized waveguide mode is about 0.01% of the total focused beam energy. This poor collection efficiency is mostly caused by the inefficient excitation of a longitudinal field at the tip apex from far-field (by the free-space focused beam). The propagation loss of the SPP and the excitation efficiency of the fiber mode by coupling to the conical SPP also contribute to the total collection efficiency (for losses, see Supporting Information, S1). Meanwhile, when the light is coupled to the fiber and emitted through the tip, the measured conversion efficiency is ≈0.3% while the theoretical estimation is ≈0.53% (formula 5 in Supporting Information, S1).

DISCUSSION

We demonstrated, with our experimental study, the excitation of the radially polarized SPP in a plasmonic tip (tapered and fully metal coated M-profile fiber), which works as a conical Kretschman configuration. The excitation process is based on the resonant coupling of the radially polarized WG mode of an M-profile fiber to the radially polarized SPP on the conical metal layer covering the tapered fiber. The SPP gets localized at the nanoscale apex producing a strong longitudinal field oscillating along the tip axis.

We found that the plasmonic tip apex, due to the longitudinal localized field at the apex, emits to the side. To probe the near-field characteristics at the tip apex, we placed the tip vertically on a planar metal surface and studied the planar SPPs generated on the metal surface by the plasmonic tip. The planar SPPs, originating from the position of the tip, propagate to all radial directions on the planar surface. By scattering SPPs with a grating, we measured the scattered beam, which was shown to be radially polarized and radially symmetric. With this experiment, we showed that the radially polarized WG mode in

DOI: 10.1021/acsphotonics.5b00339
ACS Photonics 2015, 2, 1468−1475

an M-profile fiber-based plasmonic tip generates a longitudinal field at the apex via intermediate conical SPP excitation. We also demonstrated the reverse process: an induced longitudinal field at the plasmonic tip apex produces radially polarized WG mode in the fiber via SPP excitation originating from the tip apex. A focused laser beam generates a longitudinal field at the plasmonic tip apex, which serves as a source of conical SPPs. The conical SPPs in turn excite the WG mode in the fiber due to the resonant coupling. Polarization-resolved measurements proved that the fiber output is radially polarized; consequently, the conical SPPs, which excited the WG mode, are also radially polarized. By imaging a free space focused beam with the plasmonic tip, we found that the tip decouples the longitudinal and transversal fields; thus, the plasmonic tip can be used to individually detect the intensities of three orthogonal field components of the near-field simultaneously.

In summary, the plasmonic tip excites SPPs by its geometry from a WG mode and confines them at the nanoscale apex, and the calculations show that this energy conversion process is quite efficient. In the collection mode, the tip detects the light polarized along the tip axis (longitudinal field) despite being an apertureless tip. In the scattering mode, the plasmonic tip detects the transversal field. Potentially, the plasmonic tip can efficiently excite and detect the near-field with strongly suppressed background noise. Hence, by combining the best features of apertureless and aperture SNOM tips, the plasmonic tip promises to be a very good candidate for a SNOM tip with higher conversion efficiency from far-field to near-field than conventional tips. To realize the full potential of the plasmonic tip, it is necessary to develop a technology for sharpening the metallic tip apex that would then allow us to have enhanced topographical and optical resolution. In conclusion, with our experimental study, we expanded the well-known Kretschmann configuration to the conical geometry and employed the plasmonic tip that can be used as an SNOM tip for sensing the longitudinal and transversal field components individually.

METHODS

Coupling of a Radially Polarized Beam into a Plasmonic Tip Fiber. We generate a radially polarized beam from a Gaussian beam (continuous wave laser operating at 784 nm) with a radial polarization converter (ArcOptix) in free space. To reliably deliver a radially polarized free space beam into the fiber with the plasmonic tip, we use a piece of intermediate M-profile fiber. First, the free-space beam is coupled into the intermediate M-profile fiber via an aspheric lens (Supporting Information, Figure S4a). Then, we ensure that the output of this fiber is radially polarized by recording the output beam profile at different orientations of a polarization analyzer that is placed in front of a CCD beam profiler. Afterward, the facets of the intermediate M-profile fiber and the plasmonic tip M-profile fiber are spliced. In separate experiments (not presented here), we determined the splicing parameters that allow transmission of the TM_{01} (radially polarized) mode through the spliced region with high modal purity. On average, about 3.5 mW power is coupled to the plasmonic tip fiber with coating thickness of about 130 nm.

In a symmetrically and adiabatically tapered plasmonic tip, the radially polarized WG mode should conserve its polarization state and should not couple to fundamental or higher order WG modes.[49,50] We explored the polarization state of the guided mode within the tapered region of the plasmonic tip by cross-sectioning the tip's end with a focused ion beam (FIB) and observing the transmitted beam. The transmission pattern of the cross-sectioned plasmonic tip shows that the mode is preserved down to an outer diameter of the fiber of 3 μm, with only slight disturbances in the intensity profile (Supporting Information, Figure S4b). We examined the mode's polarization state by measuring the intensity profile at different orientations of the polarization analyzer, and the measurements confirmed that the mode is radially polarized. This result assures that the tapered fibers, which we use in our experiments, can guide the radially polarized mode with negligible distortion.

Near-Field Analysis of a Plasmonic Tip Apex. The near-field of the plasmonic tip apex was analyzed with the setup presented in Figure 3a. A tuning-fork-based SNOM operating in shear-force feedback mode (NtegraSolaris, NT-MDT) is employed to position the plasmonic tip in the center of the disc and to control the distance between the tip apex and the disk surface.

The bull's eye grating, serving as a screen for observing the planar SPPs via scattering, was fabricated on a 150 nm gold layer deposited on a glass coverslip. It consists of a disk with a diameter of 6.5 μm and five annular slits with a period of 765 nm (equal to the SPP wavelength) surrounding the disk, which are milled by a focused ion beam (FIB) through the entire gold thickness. The SPPs, excited in the middle of the disk, propagate outward and are scattered by the slits into free-space waves propagating perpendicular to the sample plane. The real-space image of the scattered light from the other side of the grating (metal/glass interface) is recorded on a CCD attached to an inverted microscope (presented in the lower part of Figure 3a) with a total magnification of 50 (consisting of an objective with 20× and an axillary lens with 2.5×).

Detection with a Plasmonic Tip via Radially Polarized Conical SPP. The reverse resonant excitation process (energy transfer from the radially polarized conical SPP into the waveguide mode of the fiber) is analyzed with a setup that is sketched in Figure 4a. The plasmonic tip is handled in a tip-scanning SNOM (NtegraSolaris, NT-MDT), and a free-space beam is focused with a 100×, NA = 0.75 objective (Zeiss), which can be translated in the axial direction with the help of a nanopositioning piezo stage (PIFOC, Physik Instrumente GmbH). The tip scans in the horizontal plane (xy) and signals are recorded with photomultiplier tubes (PMTs) and a CCD. We monitored the "transmitted" signal that is detected by the plasmonic tip and the "backscattered" signal that is collected by the focusing objective. We used about 0.3 mW laser power on average for the free-space beam in these measurements, and the signal level of the backscattered beam was below 50 nW. The tip, used in this measurement, has a coating thickness of about 100 nm.

ASSOCIATED CONTENT

Supporting Information

The Supporting Information is available free of charge on the ACS Publications website at DOI: 10.1021/acsphotonics.5b00339.

Additional experimental details (PDF).

AUTHOR INFORMATION

Corresponding Author

*E-mail: norik.janunts@uni-jena.de.

DOI: 10.1021/acsphotonics.5b00339
ACS Photonics 2015, 2, 1468−1475

Present Address

‡Laboratoire d'Optique Biomedicale, Ecole Polytechnique Federale de Lausanne, 1015 Lausanne, Switzerland.

Notes

The authors declare no competing financial interest.

■ ACKNOWLEDGMENTS

The authors acknowledge financial and facility support from the Federal Ministry of Education and Research (PhoNa, Germany), the Thuringian State Government (MeMa, Germany). We would also like to acknowledge Mr. Thomas Kaiser for motivating discussions and Prof. Siddharth Ramachandran for introducing M-profile fibers to us and for valuable discussions. We want to express our great appreciation to Prof. Khachatur Nerkararyan for discussing systematically and suggesting methods in the course of this study, which helped us to understand better and deeper the investigated phenomenon. We are thankful to Mr. Christian Hupel for refractive index measurements of the M-profile fibers.

■ REFERENCES

(1) Barnes, W. L.; Dereux, A.; Ebbesen, T. W. Surface Plasmon Subwavelength Optics. *Nature* **2003**, *424*, 824−830.

(2) Novotny, L.; van Hulst, N. Antennas for Light. *Nat. Photonics* **2011**, *5*, 83−90.

(3) Kawata, S.; Inouye, Y.; Verma, P. Plasmonics for near-Field Nano-Imaging and Superlensing. *Nat. Photonics* **2009**, *3*, 388−394.

(4) Gramotnev, D. K.; Bozhevolnyi, S. I. Plasmonics beyond the Diffraction Limit. *Nat. Photonics* **2010**, *4*, 83−91.

(5) Nerkararyan, K. Superfocusing of a Surface Polariton in a Wedge-like Structure. *Phys. Lett. A* **1997**, *237*, 103−105.

(6) Takahara, J.; Yamagishi, S.; Taki, H.; Morimoto, A.; Kobayashi, T. Guiding of a One-Dimensional Optical Beam with Nanometer Diameter. *Opt. Lett.* **1997**, *22*, 475.

(7) Babadjanyan, A. J.; Margaryan, N. L.; Nerkararyan, K. V. Superfocusing of Surface Polaritons in the Conical Structure. *J. Appl. Phys.* **2000**, *87*, 3785.

(8) Stockman, M. Nanofocusing of Optical Energy in Tapered Plasmonic Waveguides. *Phys. Rev. Lett.* **2004**, *93*.10.1103/PhysRevLett.93.137404

(9) Choo, H.; Kim, M.-K.; Staffaroni, M.; Seok, T. J.; Bokor, J.; Cabrini, S.; Schuck, P. J.; Wu, M. C.; Yablonovitch, E. Nanofocusing in a Metal−insulator−metal Gap Plasmon Waveguide with a Three-Dimensional Linear Taper. *Nat. Photonics* **2012**, *6*, 838−844.

(10) Park, I.-Y.; Kim, S.; Choi, J.; Lee, D.-H.; Kim, Y.-J.; Kling, M. F.; Stockman, M. I.; Kim, S.-W. Plasmonic Generation of Ultrashort Extreme-Ultraviolet Light Pulses. *Nat. Photonics* **2011**, *5*, 677−681.

(11) Choi, H.; Pile, D. F.; Nam, S.; Bartal, G.; Zhang, X. Compressing Surface Plasmons for Nano-Scale Optical Focusing. *Opt. Express* **2009**, *17*, 7519.

(12) Verhagen, E.; Kuipers, L. K.; Polman, A. Plasmonic Nanofocusing in a Dielectric Wedge. *Nano Lett.* **2010**, *10*, 3665−3669.

(13) Davoyan, A. R.; Shadrivov, I. V.; Zharov, A. A.; Gramotnev, D. K.; Kivshar, Y. S. Nonlinear Nanofocusing in Tapered Plasmonic Waveguides. *Phys. Rev. Lett.* **2010**, *105*, 116804.

(14) Pile, D. F. P.; Gramotnev, D. K. Adiabatic and Nonadiabatic Nanofocusing of Plasmons by Tapered Gap Plasmon Waveguides. *Appl. Phys. Lett.* **2006**, *89*, 041111.

(15) Stöckle, R. M.; Suh, Y. D.; Deckert, V.; Zenobi, R. Nanoscale Chemical Analysis by Tip-Enhanced Raman Spectroscopy. *Chem. Phys. Lett.* **2000**, *318*, 131−136.

(16) Hayazawa, N.; Yano, T.; Watanabe, H.; Inouye, Y.; Kawata, S. Detection of an Individual Single-Wall Carbon Nanotube by Tip-Enhanced near-Field Raman Spectroscopy. *Chem. Phys. Lett.* **2003**, *376*, 174−180.

(17) Hartschuh, A.; Sánchez, E.; Xie, X.; Novotny, L. High-Resolution near-Rield Raman Microscopy of Single-Walled Carbon Nanotubes. *Phys. Rev. Lett.* **2003**, *90*, 095503.

(18) Hartschuh, A.; Beversluis, M. R.; Bouhelier, A.; Novotny, L. Tip-Enhanced Optical Spectroscopy. *Philos. Trans. R. Soc., A* **2004**, *362*, 807−819.

(19) Saito, Y.; Hayazawa, N.; Kataura, H.; Murakami, T.; Tsukagoshi, K.; Inouye, Y.; Kawata, S. Polarization Measurements in Tip-Enhanced Raman Spectroscopy Applied to Single-Walled Carbon Nanotubes. *Chem. Phys. Lett.* **2005**, *410*, 136−141.

(20) Fleischer, M.; Weber-Bargioni, A.; Altoe, M. V. P.; Schwartzberg, A. M.; Schuck, P. J.; Cabrini, S.; Kern, D. P. Gold Nanocone near-Field Scanning Optical Microscopy Probes. *ACS Nano* **2011**, *5*, 2570−2579.

(21) De Angelis, F.; Das, G.; Candeloro, P.; Patrini, M.; Galli, M.; Bek, A.; Lazzarino, M.; Maksymov, I.; Liberale, C.; Andreani, L. C.; Di Fabrizio, E. Nanoscale Chemical Mapping Using Three-Dimensional Adiabatic Compression of Surface Plasmon Polaritons. *Nat. Nanotechnol.* **2010**, *5*, 67−72.

(22) Berweger, S.; Atkin, J.; Olmon, R. L.; Raschke, M. B. Adiabatic Tip-Plasmon Focusing for Nano-Raman Spectroscopy. *J. Phys. Chem. Lett.* **2010**, *1*, 3427−3432.

(23) Schmidt, S.; Piglosiewicz, B.; Sadiq, D.; Shirdel, J.; Lee, J. S.; Vasa, P.; Park, N.; Kim, D.-S.; Lienau, C. Adiabatic Nanofocusing on Ultrasmooth Single-Crystalline Gold Tapers Creates a 10-Nm-Sized Light Source with Few-Cycle Time Resolution. *ACS Nano* **2012**, *6*, 6040−6048.

(24) Bouhelier, A.; Renger, J.; Beversluis, M. R.; Novotny, L. Plasmon-Coupled Tip-Enhanced near-Field Optical Microscopy. *J. Microsc.* **2003**, *210*, 220−224.

(25) Janunts, N.; Baghdasaryan, K.; Nerkararyan, K.; Hecht, B. Excitation and Superfocusing of Surface Plasmon Polaritons on a Silver-Coated Optical Fiber Tip. *Opt. Commun.* **2005**, *253*, 118−124.

(26) Barthes, J.; Colas des Francs, G.; Bouhelier, A.; Dereux, A. A Coupled Lossy Local-Mode Theory Description of a Plasmonic Tip. *New J. Phys.* **2012**, *14*, 083041.

(27) Ding, W.; Andrews, S.; Maier, S. Internal Excitation and Superfocusing of Surface Plasmon Polaritons on a Silver-Coated Optical Fiber Tip. *Phys. Rev. A: At., Mol., Opt. Phys.* **2007**, *75*.10.1103/PhysRevA.75.063822

(28) Tortora, P.; Descrovi, E.; Aeschimann, L.; Vaccaro, L.; Herzig, H.-P.; Dändliker, R. Selective Coupling of HE11 and TM01 Modes into Microfabricated Fully Metal-Coated Quartz Probes. *Ultramicroscopy* **2007**, *107*, 158−165.

(29) Frey, H. G.; Bolwien, C.; Brandenburg, A.; Ros, R.; Anselmetti, D. Optimized Apertureless Optical near-Field Probes with 15 Nm Optical Resolution. *Nanotechnology* **2006**, *17*, 3105−3110.

(30) Chen, X.-W.; Sandoghdar, V.; Agio, M. Highly Efficient Interfacing of Guided Plasmons and Photons in Nanowires. *Nano Lett.* **2009**, *9*, 3756−3761.

(31) Eckert, R.; Freyland, J. M.; Gersen, H.; Heinzelmann, H.; Schürmann, G.; Noell, W.; Staufer, U.; de Rooij, N. F. Near-Field Fluorescence Imaging with 32 Nm Resolution Based on Microfabricated Cantilevered Probes. *Appl. Phys. Lett.* **2000**, *77*, 3695.

(32) Ramachandran, S.; Kristensen, P.; Yan, M. F. Generation and Propagation of Radially Polarized Beams in Optical Fibers. *Opt. Lett.* **2009**, *34*, 2525.

(33) Kretschmann, E. Die Bestimmung optischer Konstanten von Metallen durch Anregung von Oberflächenplasmaschwingungen. *Eur. Phys. J. A* **1971**, *241*, 313−324.

(34) Novotny, L.; Hafner, C. Light Propagation in a Cylindrical Waveguide with a Complex, Metallic, Dielectric Function. *Phys. Rev. E: Stat. Phys., Plasmas, Fluids, Relat. Interdiscip. Top.* **1994**, *50*, 4094−4106.

(35) Esmann, M.; Becker, S. F.; da Cunha, B. B.; Brauer, J. H.; Vogelgesang, R.; Groß, P.; Lienau, C. K-Space Imaging of the Eigenmodes of Sharp Gold Tapers for Scanning near-Field Optical Microscopy. *Beilstein J. Nanotechnol.* **2013**, *4*, 603−610.

DOI: 10.1021/acsphotonics.5b00339
ACS Photonics 2015, 2, 1468−1475

(36) Pfeiffer, C.; Economou, E.; Ngai, K. Surface Polaritons in a Circularly Cylindrical Interface: Surface Plasmons. *Phys. Rev. B* **1974**, *10*, 3038−3051.
(37) Atomic Force Microscopy for Nanotechnology and Scientific Research | NT-MDT, http://www.ntmdt.com/ (accessed Jun 12, 2015).
(38) NSOM/SNOM, TERS, Low Temperature AFM & SPM Solutions from Nanonics, http://www.nanonics.co.il/ (accessed Jun 12, 2015).
(39) Rakic, A. D.; Djurišic, A. B.; Elazar, J. M.; Majewski, M. L. Optical Properties of Metallic Films for Vertical-Cavity Optoelectronic Devices. *Appl. Opt.* **1998**, *37*, 5271.
(40) Proietti Zaccaria, R.; Alabastri, A.; De Angelis, F.; Das, G.; Liberale, C.; Toma, A.; Giugni, A.; Razzari, L.; Malerba, M.; Sun, H. B.; Di Fabrizio, E. Fully Analytical Description of Adiabatic Compression in Dissipative Polaritonic Structures. *Phys. Rev. B: Condens. Matter Mater. Phys.* **2012**, *86*, 035410.
(41) Ropers, C.; Neacsu, C. C.; Elsaesser, T.; Albrecht, M.; Raschke, M. B.; Lienau, C. Grating-Coupling of Surface Plasmons onto Metallic Tips: A Nanoconfined Light Source. *Nano Lett.* **2007**, *7*, 2784−2788.
(42) Dorn, R.; Quabis, S.; Leuchs, G. Sharper Focus for a Radially Polarized Light Beam. *Phys. Rev. Lett.* **2003**, *91*, 233901.
(43) Mueller, J. P. B.; Capasso, F. Asymmetric Surface Plasmon Polariton Emission by a Dipole Emitter near a Metal Surface. *Phys. Rev. B: Condens. Matter Mater. Phys.* **2013**, *88*, 121410.
(44) Richards, B.; Wolf, E. Electromagnetic Diffraction in Optical Systems. II. Structure of the Image Field in an Aplanatic System. *Proc. R. Soc. London, Ser. A* **1959**, *253*, 358−379.
(45) Youngworth, K.; Brown, T. Focusing of High Numerical Aperture Cylindrical-Vector Beams. *Opt. Express* **2000**, *7*, 77.
(46) Yew, E. Y. S.; Sheppard, C. J. R. Tight Focusing of Radially Polarized Gaussian and Bessel-Gauss Beams. *Opt. Lett.* **2007**, *32*, 3417.
(47) Betzig, E.; Chichester, R. J. Single Molecules Observed by Near-Field Scanning Optical Microscopy. *Science* **1993**, *262*, 1422−1425.
(48) Gersen, H.; García-Parajó, M. F.; Novotny, L.; Veerman, J. A.; Kuipers, L.; Van Hulst, N. F. Near-Field Effects in Single Molecule Emission. *J. Microsc.* **2001**, *202*, 374−378.
(49) Jung, Y.; Brambilla, G.; Richardson, D. J. Broadband Single-Mode Operation of Standard Optical Fibers by Using a Sub-Wavelength Optical Wire Filter. *Opt. Express* **2008**, *16*, 14661.
(50) Ravets, S.; Hoffman, J. E.; Kordell, P. R.; Wong-Campos, J. D.; Rolston, S. L.; Orozco, L. A. Intermodal Energy Transfer in a Tapered Optical Fiber: Optimizing Transmission. *J. Opt. Soc. Am. A* **2013**, *30*, 2361−2371.

DOI: 10.1021/acsphotonics.5b00339
ACS Photonics 2015, 2, 1468−1475